Contents lists available at ScienceDirect

Virology

journal homepage: www.elsevier.com/locate/yviro

VIROLOGY

Moloney murine leukemia virus decay mediated by retroviral reverse transcriptase degradation of genomic RNA

Monica Casali [a,c,*], Carlo Zambonelli [b], Jonathan Goldwasser [a], Halong N. Vu [a], Martin L. Yarmush [a,c,*]

[a] Center for Engineering in Medicine/Department of Surgery, Massachusetts General Hospital, Shriners Burns Hospital, Harvard Medical School, Boston, MA 02114, USA
[b] Molecular and Cellular Biology Department, Harvard University, Cambridge, MA 02138, USA
[c] Biomedical Engineering Department, Rutgers University, Piscataway, NJ 08854, USA

ABSTRACT

Retroviral vectors are powerful tools for the introduction of transgenes into mammalian cells and for long-term gene expression. However, their application is often limited by a rapid loss of bioactivity: retroviruses spontaneously loose activity at 37 °C, with a half-life of 4 to 9 h depending on the retrovirus type. We sought to determine which components of the retrovirus are responsible for this loss in bioactivity and to obtain a quantitative characterization of their stability. To this end, we focused on RNA and viral proteins, two major components that we hypothesized may undergo degradation and negatively influence viral infectivity. Reverse transcription PCR (RT-PCR) targeting RNA encoding portions of the viral genome clearly demonstrated time-dependent degradation of RNA which correlated with the loss in viral bioactivity. Circular dichroism spectroscopy, SDS-PAGE and two-dimensional SDS-PAGE analyses of viral proteins did not show any change in secondary structure or evidence of proteolysis. The mechanism underlying the degradation of viral RNA was investigated by site-directed mutagenesis of proteins encoded by the viral genome. Reverse transcriptase and protease mutants exhibited enhanced RNA stability in comparison to wild type recombinant virus, suggesting that the degradation of RNA, and the corresponding virus loss of activity, is mediated by the reverse transcriptase enzyme.

© 2008 Elsevier Inc. All rights reserved.

Introduction

Retroviral vectors have been widely used in gene therapy applications (Gordon and Anderson, 1994; Pages and Bru, 2004), including the first successful gene therapy protocol for X-linked severe combined immunodeficiency (SCID-X1) (Aiuti et al., 2002; Cavazzana-Calvo et al., 2000). Retroviruses have several advantages over other vectors, including the ability to permanently modify the nuclear genome of the host, the relative simplicity of the retroviral genome and ease of use (Barquinero, Eixarch, and Perez-Melgosa, 2004; Kohn et al., 2003; Mitani, Wakamiya, and Caskey, 1993; Relph, Harrington, and Pandha, 2004; Robbins and Ghivizzani, 1998). Since the first gene therapy clinical trials in the early 1990's, Moloney murine leukemia virus (MMuLV)-based vectors have been the preferred tool for stable genetic modification. A total of 254 clinical trials have relied on this type of vector, accounting for 28% of the total number of viral gene therapy clinical trials approved world-wide (Barquinero, Eixarch, and Perez-Melgosa, 2004; Kohn et al., 2003; Relph, Harrington, and Pandha, 2004).

Among the requirements for successful gene therapy, highly efficient delivery of genetic material and stability of the gene carrier are indispensable. One problem limiting successful clinical application of MMuLV-based vectors is inefficient gene transfer. This inefficiency is attributable to several factors: (a) murine gamma-retroviruses infect only actively dividing cells (Miller, Adam, and Miller, 1990; Roe et al., 1993), (b) murine gamma-retroviruses are rapidly inactivated by the human complement system (Chuck, Clarke, and Palsson, 1996; Takeuchi et al., 1996) and (c) virions have a short half-life of 4–9 h, limiting viral stability and titer (Chuck, Clarke, and Palsson, 1996; Le Doux et al., 1999; Merten et al., 2001). Most research on murine gamma-retrovirus-mediated gene transfer has focused on the development of vector constructs and packaging cell lines and optimization of the delivery process (Daly and Chernajovsky, 2000; Davis, Morgan, and Yarmush, 2002; Davis et al., 2004; Hanenberg et al., 1996; Le Doux et al., 1999). Efforts have been made to address retroviral vector shortcomings by improving viral titers via concentration processes (Paul et al., 1993; Pham et al., 2001; Reeves and Cornetta, 2000), producing retrovirus at a low temperature to decelerate the rate of decay (Kotani et al., 1994; Kwon and Peng, 2005), engineering packaging cells to produce retroviruses resistant to inactivation by human serum (Cosset et al., 1995; Mason et al., 1999; Pensiero et al., 1996) and removing transduction inhibitors secreted by the packaging cell lines (Le Doux et al., 1996; Le Doux, Morgan, and Yarmush, 1998 Le Doux";,1999).

* Corresponding authors. 51 Blossom Street, Room 417, Boston, MA 02114, USA. Fax: +1 617 573 9471.
E-mail addresses: mcasali@hms.harvard.edu (M. Casali), ireis@sbi.org (M.L. Yarmush).

Despite that retrovirus applications to gene therapy suffer significant limitations imposed by viral instability at physiological temperature (Kotani et al., 1994; Le Doux et al., 1999) the mechanism by which decay occurs is still unclear. The three components that can undergo degradation are the membrane enveloping the virus, the protein component and the nucleic acid. Previous studies showed that viral envelop lipid composition and lipid oxidation affect viral stability (Poryvaev, 1995, 1996; Poryvaev and Zykova, 1995) and in a recent study Beer et al. (2003) showed that high cholesterol levels in the viral lipid shell decrease thermal viral stability.

Here we investigate the stability of the viral RNA and capsid proteins using biophysical and molecular techniques. Based on our observations, we propose a mechanism for the decay of MMuLV-derived vectors involving the viral reverse transcriptase.

Results

Viral RNA decays on a time scale similar to that of the loss in bioactivity

In order to examine possible relationships between retroviral decay and decay of viral components, we began by examining the stability of the viral RNA. Solutions of MMuLV-based vector were incubated at 37 °C and 4 °C and samples were collected at different time points and stored at −80 °C. RNA was isolated and analyzed by
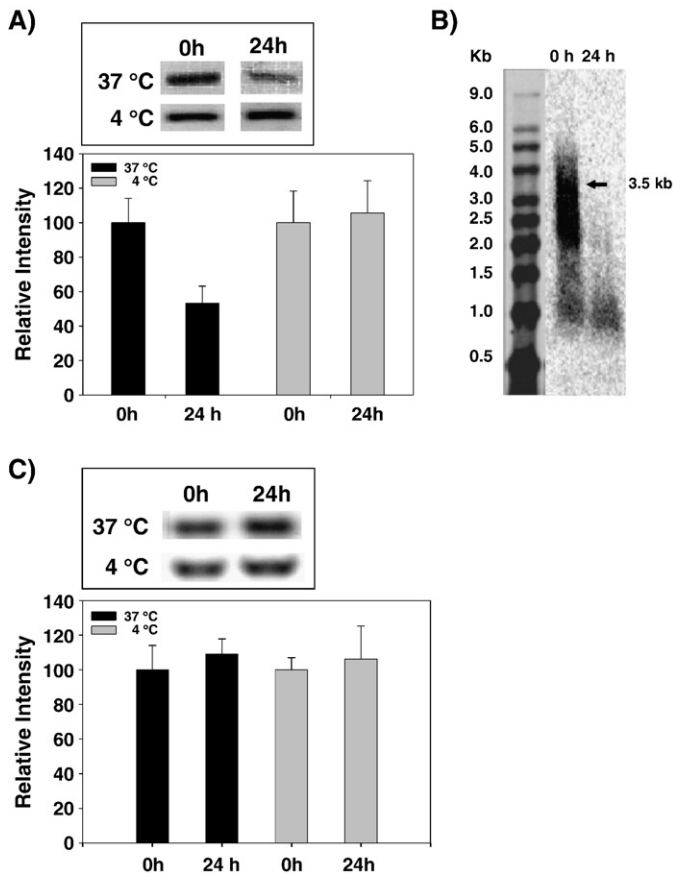

Fig. 1. End point RT-PCR analysis (A), and Northern blot (B) of retroviral RNA decay. Virus was incubated at 37 °C and 4 °C. RT-PCR was performed on samples collected at 0 and 24 h, and products were analyzed on agarose gel and stained with SYBR Green. Representative data from 3 decay experiments are shown. Northern blot analysis was performed on virus samples incubated at 37 °C and collected at 0 and 24 h. End point RT-PCR for the endogenous reverse transcription (C).Virus was incubated at 37 °C and 4 °C. RT-PCR was performed on samples collected at 0 and 24 h and products were analyzed on agarose gel and stained with SYBR Green. Representative data from 3 experiments are shown. The arrow in (B) indicates the size of the intact RNA genome.
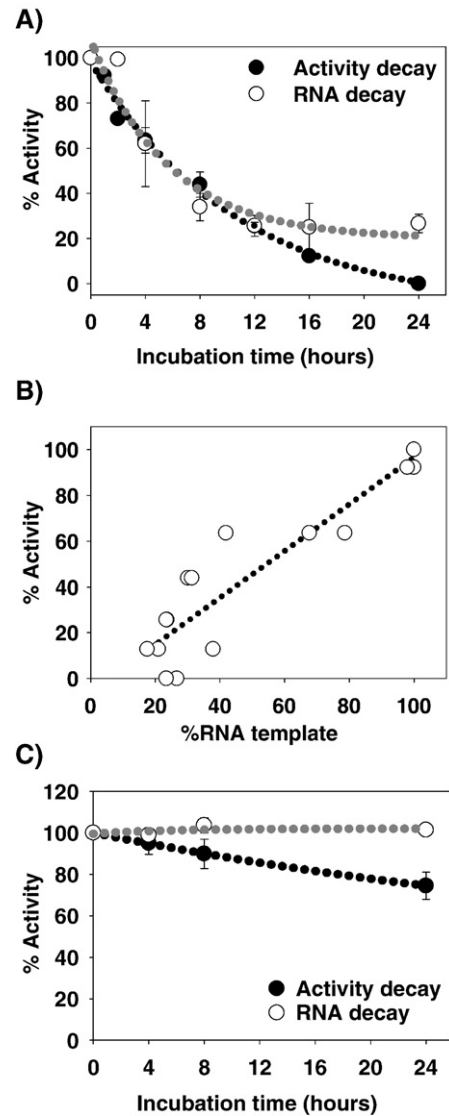

Fig. 2. Quantitative analysis of RNA decay and viral bioactivity. Virus was incubated at (A) 37 °C and (C) 4 °C; samples were collected at different intervals of time for analysis by real time RT-PCR and transduction assays. RNA integrity and viral bioactivity (data obtained from panel (A)) were linearly correlated (r^2=0.99). Data points in A and C are mean±standard deviation, n=3. Data points in B are mean activity values and RNA integrity values for each time point from 3 experiments.

end point RT-PCR with primers directed at the LacZ region. End point data clearly showed a decrease in the intensity of amplified RNA as a function of time for the virus incubated at 37 °C, but not for the samples incubated at 4 °C (Fig. 1A). Northern blot analysis (Fig. 1B) confirmed the degradation of RNA at 37 °C. After 24 h incubation, no high molecular weight RNA was visible and the overall signal intensity of the viral RNA decreased as well. The possibility that Natural Endogenous Reverse Transcription (NERT) is responsible for viral RNA degradation was investigated at 37 °C and 4 °C at different time points (Fig. 1C). No significant increase of NERT products were found after 24 h incubation at neither temperatures.

Analysis of viral RNA integrity by real time PCR demonstrated exponential decay at 37 °C (Fig. 2A). The rate of RNA decay was similar to the rate of loss in viral bioactivity as measured by LacZ transduction assays (Fig. 2A), with a linear correlation (r^2=0.99) between the two (Fig. 2B). When the virus was incubated at 4 °C, no measurable RNA decay occurred, while a slight (20%) loss in viral bioactivity over 24 h was observed (Fig. 2C). Similar results were obtained using primers specific for the viral *gag* region (data not shown).

A) D27N (PR⁻)

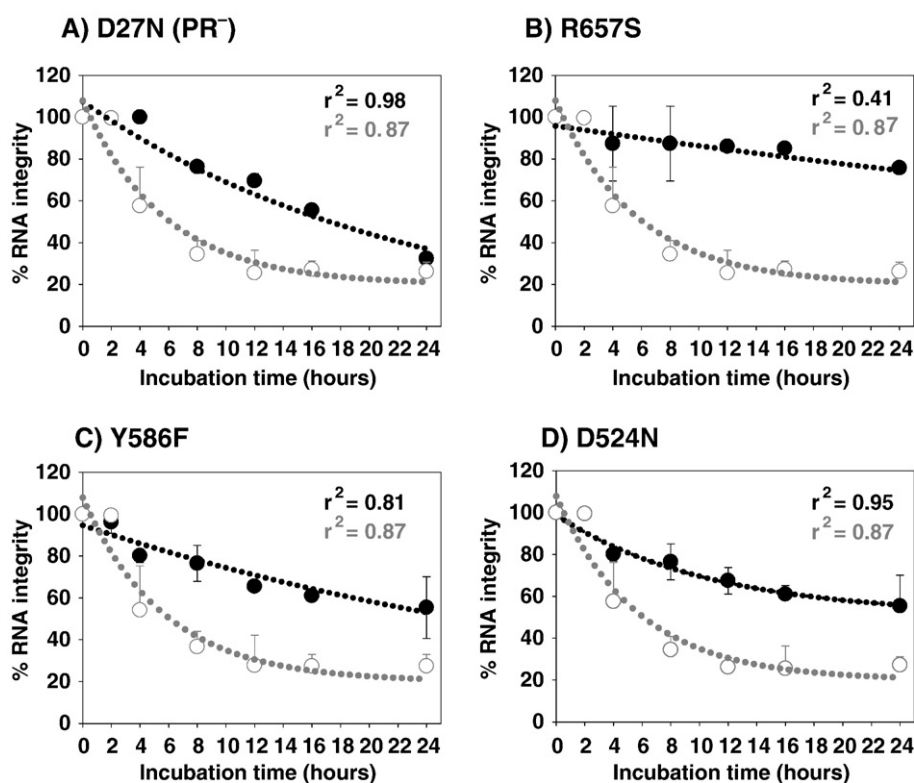## B) R657S

C) Y586F

D) D524N

Fig. 3. RNA decay in protease (A), and reverse transcriptase mutants (B–D). Virus samples were incubated at 37 °C, and samples were collected at different time intervals of time and analyzed by real time RT-PCR. All mutants exhibit enhanced RNA stability compared to the wild type virus (in gray). Data points represent mean±standard deviation, $n=3$.

Protease and reverse transcriptase mutants exhibit enhanced RNA stability

Protease and reverse transcriptase mutants were obtained by site-directed mutagenesis on pVPack-GP plasmid. Wild type virus was obtained from transient transfection under the same conditions as the mutants, and the wild type virus produced under both stable and transient conditions showed the same bioactivity and decay kinetic. Despite that retroviral proteases share limited amino acid homology with members of the aspartyl protease family, the active site residues Asp-Thr-Gly are highly conserved. Substitution of the aspartic acid residue at position 27 of MMuLV protease with asparagine (D27N) abrogates protease activity, inhibiting viral maturation and infectivity, while maintaining the ability to form immature (uncondensed) virus particles (Fu et al., 2006; Fu and Rein, 1993; Kohl et al., 1988).

Reverse transcriptase mutants were previously described by Blain and Goff (1993); in these mutants DNA–RNA (*RNase H*) and RNA–RNA (*RNase H**) nuclease activities of the viral reverse transcriptase were functionally separated. Based on the cited work we produced three viral mutants: mutation R657S which selectively reduced RNase H* but not RNase H activity; mutation Y586F which abolished RNase H activity, but not RNase H* activity; and mutation D524N which reduced both RNase H and RNase H* activities, as compared to the wild type enzyme. RNA degradation in the mutant viruses was investigated over a period of 24 h by end point and real time RT-PCR and compared to the wild type virus. All mutants exhibited a slower rate of RNA degradation than wild type. The protease mutant displayed linear RNA degradation kinetics, with approximately 50% RNA degradation after 18 h, instead of the 6 h observed for the wild type virus, and 30 to 40% RNA integrity remaining at 24 h (Fig. 3A). Mutant R657S retained 80% of its RNA integrity after 24 h (Fig. 3B), while Y585F and D524N retained 60% and 70% of their initial RNA integrity at 24 h, respectively (Figs. 3C, D). We have not yet been able

to correlate the RNA degradation results to viral bioactivity data for mutant nucleases. This could be because the mutants are not infective, or their titer is not sufficient.

Retroviral proteins are stable over a 13 h period at 37 °C

To investigate the stability of retroviral proteins, we employed two techniques: far and near UV CD spectroscopy measurements were performed to detect large changes in the secondary structure of the viral proteins, while SDS-PAGE and 2D-PAGE were utilized to monitor non specific degradation or specific cleavage of the proteins. The quality of the samples for CD analysis was confirmed by SDS-PAGE and contaminating bands were negligible. CD spectra contained a negative peak at approximately 217 nm, indicating beta-sheet structure, and a peak at 290 nm, corresponding to aromatic amino acids. Retrovirus was incubated at 37 °C for 13 h, and CD spectra were collected every hour. No major change in intensity or position was observed for either peaks over a 13 h period at 37 °C (Fig. 4A). Degradation of viral proteins was investigated by SDS-PAGE (Fig. 4B) and 2D-PAGE (data not shown). No changes in protein patterns were detected for retrovirus incubated at 37 °C for up to 24 h, indicating that viral proteins did not degrade over this time period.

Discussion

The decay of retroviral activity is a significant factor contributing to the inefficiency of retroviruses as vectors for gene transfer. Since these vectors are non-replicating, only two functions of the retroviral life cycle are critical for the success of a therapeutic protocol: first, the viral interaction with the host cell surface and introduction of the viral genome into the cell; and second, the integration of the viral genome into the cellular genome and expression of viral proteins by the host cell. Throughout both of these steps the integrity of the viral envelope, viral proteins and genomic material is essential: degradation of one or
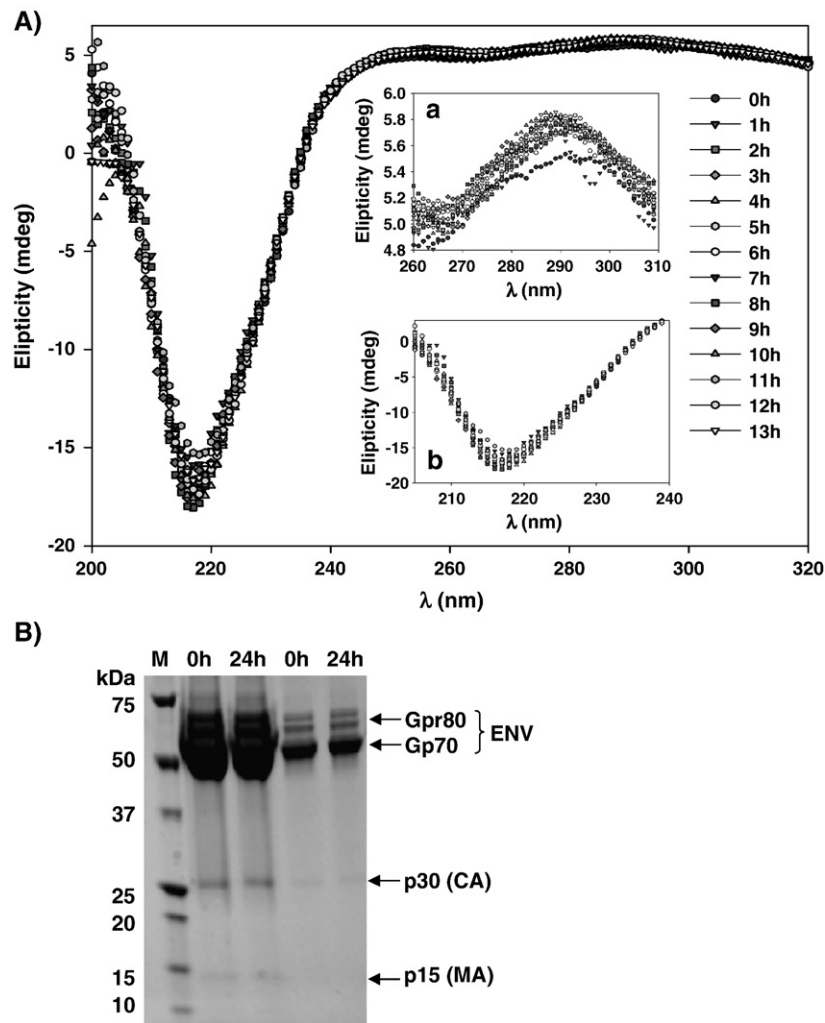
A)

B)

Fig. 4. (A) CD spectra of viral particles incubated at 37 °C over 13 h. No changes in the shape and intensity of the spectra are observed. Detail of (a) aromatic region, and (b) beta-sheet region confirm no changes in the spectra. (B) SDS-PAGE analysis of viral protein at 0 h and after 24 h of incubation at 37 °C. In the two sample sets different amounts were loaded to show high and low abundance proteins. Only major viral proteins as envelope (ENV), capsid (CA) and matrix (MA) are visible and no degradation is detectable. Other viral proteins are not visible because these are too small or poorly represented.

all of these components may be responsible for the rapid decay in viral bioactivity. Studies reporting the effect of envelope lipid composition and oxidation on virus stability have been previously published, but no investigation on viral genome and protein stability has yet been reported. To better understand the mechanism underlying retroviral decay we investigated the stability of the retroviral RNA and proteins.

We first investigated the stability of viral RNA by end point and real time RT-PCR and northern blot. Despite that PCR analysis only targets a small region of the genome, degradation of this segment reflects the loss of total genomic RNA; we consider the amount of RNA template present at time 0 h to be 100%, while the residual template amount at 24 h is expressed as a percentage of the initial amount. This assumption is essential to understand the apparent discrepancy observed between PCR and transduction assays. Our data show a decrease in RNA template over 24 h when the virus was incubated at 37 °C but not at 4 °C (Fig. 1A). The same kinetic profile (Fig. 1B) and the linear correlation (Fig. 2B) found between viral activity, as measured by transduction assays, and RNA template amount, measured by real time PCR experiments, strongly suggests that RNA degradation contributes to decay. Northern blot data (Fig. 1B) clearly show degradation of viral RNA (corresponding to an intact genome of 3.5 kb). After 24 h incubation of the virus particles at 37 °C high molecular weight RNA molecules are not detected, and the decrease of the signal intensity suggests that a complete degradation of RNA has

also occurred. At 0 h, despite that full length genomic RNA of 3.5 kb is detectable (Fig. 1B, black arrow), partial RNA degradation is visible; this degradation can be accounted for by the RNA purification process and by the fact that the 0 h sample derives from multiple virus harvests and it is a mixture of viral particles that spent up to 16 h at 37 °C. We also investigated a possible role for NERT in RNA degradation using PCR analysis. The data shows no significant amount of DNA is produced by NERT after 24 h incubation (Fig. 1C) at both temperatures.

Inside of viral particles, RNA degradation can be the result of endogenous or exogenous RNase activity (Garret and Grisham, 1995), or some combination thereof. Endogenous RNase activity can be attributed to the viral reverse transcriptase (RT), while exogenous activity may be ascribed to cellular RNase encapsulated in the virus during budding. Reverse transcriptase retro transcribes RNA to form a RNA–DNA hybrid using two separate enzymatic activities: a DNA polymerase activity, which is capable of using either RNA or DNA as a template; and a ribonuclease H activity, which degrades the viral genomic RNA in the newly synthesized RNA–DNA hybrid (Goff, 1990; Jacobo-Molina and Arnold, 1991). RNase H was thought to degrade RNA only when present in a RNA–DNA hybrid (RNase H activity); however, it was shown that MMuLV RT is capable of degrading RNA found in a RNA–RNA duplex form (RNase H* activity) (Ben-Artzi et al., 1992).

To investigate the role of the viral RT in RNA degradation we created D27N, a MMuLV protease mutant (PR⁻) whose proteolytic activity is suppressed. Virus containing the PR⁻ mutant does not mature and active viral RT is not produced by proteolytic processing of Gag-Pol (Kohl et al., 1988; Traktman and Baltimore, 1982; Witte and Baltimore, 1978). This mutant maintained 40% RNA integrity after 24 h, with degradation kinetics that were qualitatively different from wild type (Fig. 3A). While the wild type viral RNA decayed exponentially, the PR⁻ mutant appeared to decay at a constant rate. The fact that 1) there exists a lack of enzymatic activity in the PR⁻ mutant, 2) that the viral genome exists in a different conformation (D'Souza and Summers, 2004; Hibbert and Rein, 2005; Murti, Bondurant, and Tereba, 1981), and 3) that the decay rate is constant, all suggest that the mechanism for RNA degradation in the PR⁻ mutant is different from that of wild type. On the basis of these observations, we can hypothesize two different scenarios for RNA degradation: 1) that the reverse transcriptase in the non-mature virus has little or no activity and that exogenous RNases are responsible for RNA degradation; or 2) that the lower amount of secondary structure in the RNA of non-mature virus prevents the viral RNA from becoming a target of RNase H* activity within the viral RT; also in this case, exogenous RNase may be responsible for the viral RNA degradation seen in this mutants. Important is the fact that non-mature viral particles are more permeable to exogenous molecules compared to mature particles, therefore exogenous RNase can have access to the genomic RNA.

Our observations are in agreement with recent findings by Vu et al. (2007): in this study MMuLV mutant with an extended half-life (24 h instead of 5–6 h) was created by directed evolution. The mutation responsible for the enhanced half-life was mapped to the viral protease where a glycine was substituted with a glutamic acid. The researchers did not investigate the mechanism underlying the increased half-life, but, in line with our hypothesis, the mutation may have modified the substrate specificity or proteolytic efficiency of the viral protease. In either case, it is possible that viral maturation was slower compared to wild type thus yielding a more stable virus.

Mutants of the viral RT with altered substrate specificities were created and characterized by Blain and Goff (1993). Through mutational studies, the researchers functionally separated the DNA–RNA and the RNA–RNA RNase activities of the enzyme, yielding reverse transcriptase mutants with variable levels of each of these activities. To investigate a possible role for the RNase H and RNase H* activities in RNA decay, we produced three virus mutants: R657S, Y586F, and D524N. Mutant R657S has RNase H activity comparable to the wild type, but less than 1% of the wild type RNase H* activity; mutant Y586F has 5% of the wild type RNase H activity and 100% RNase H* activity; and mutant D524N has 10–25% of the wild type RNase H activity and less than 1% of RNase H* activity.

The rate of RNA decay in each mutant was quantified by real time RT-PCR after incubation at 37 °C up to 24 h (Fig. 3). All mutants exhibited a decreased rate of RNA degradation, with the R657S and D524N mutants each retaining approximately 80% RNA integrity at 24 h, while mutant Y586F retained 60% RNA integrity. These results clearly demonstrate that abrogation of RNase H* (R657S, D524N) activity enhances the stability of the viral genome. The higher RNA stability found in Y586F mutant can be the result of a lower ability of this enzyme to bind the substrate. A crystal structure of a wild type enzyme complexed with a DNA–RNA hybrid showed that Y586 binds the phosphate group of the DNA strand in the DNA–RNA hybrid (Lim et al., 2006). Likely, a similar interaction is established with the phosphate group in the RNA–RNA pairing. These data suggest also that the two enzymatic activities RNase H and RNase H* are tightly connected, as it should be expected, and mutations in one affect the other.

Our data suggest that the RNase activity of the viral RT plays a role in viral RNA degradation. In the immature virion, the two copies

of the RNA genome form a fragile dimer that becomes more stable during maturation because of an increment of kissing loops and in the secondary structure (Fu et al., 2006; Riggin, Bondurant, and Mitchell, 1975). However, this increment in the secondary structure may also make the RNA more vulnerable to the RNase H* activity from the viral RT.

We ruled out that degradation of viral proteins is responsible for the observed drop in viral infectivity. To probe protein stability during viral decay we examined the stability of the virus protein components by CD spectroscopy and SDS-PAGE. CD spectroscopy quantifies the secondary structure of proteins and small changes in secondary structure content can be detected (Cantor and Schimmel, 1980). CD spectroscopy has previously been used to study the temperature-induced decay of the Respiratory Syncytial Virus (Ausar et al., 2007; Ausar et al., 2005). CD spectra of purified virus particles showed no changes during incubation at 37 °C for a period of 13 h (Fig. 4A). This lack of variation in the CD spectrum suggests that no significant changes occurred in protein secondary structure under these conditions. It should be noted that although RNA also has a characteristic CD spectrum, which could partially overlap with the protein spectrum, RNA in the virus is present at much lower quantities than protein and no interference can be expected. The CD spectra obtained are the sum of the contribution of each individual viral protein, but different proteins contribute differently to the spectra depending on their abundance. The most represented proteins are the glycoprotein gp70 and the capsid protein p30 and they should be considered the major player in CD spectra variation, or lack of it, as it is in this case. SDS-PAGE (Fig. 4B) and two-dimensional SDS-PAGE analyses (data not shown) confirmed that protein degradation does not occur after 24 h at 37 °C, as no change was observed in the gel pattern. Our observations do not include proteins as trans-membrane (TM), nucleocapsid (NC) proteins, the polymerase and the integrase, because of the small molecular weight and/or their low abundance.

Our work demonstrates that MMuLV-derived vector activity decay is correlated with viral RNA degradation and virus particle maturation. We demonstrated that viral RNA degradation is mediated by the viral reverse transcriptase through its RNase H* activity, and mutations at the RNaseH catalytic site affects RNA stability kinetic.

Our findings suggest that it may be possible to produce a more stable MMuLV-derived retroviral vector by controlling the rate of viral maturation or eliminating enzymatic degradation of genomic RNA in the mature particles. Another interesting possibility would be to create a MMuLV with enhanced natural endogenous reverse transcription where viral RNA is retro-transcribed to DNA (Zhang et al., 1995) soon after virus budding and maturation producing a more stable DNA–RNA hybrid.

Materials and methods

Cell culture and virus harvesting

NIH 3T3 cells (ATCC CRL-1658), the amphotropic packaging cell line Ψ-CRIP (kindly provided by L.K. Cohen of Somatix Therapy Corporation, Alameda, California), which contains a MMuLV-derived vector carrying the LacZ gene and produces the α-SGC-LacZ virus (Danos and Mulligan, 1988; Price, Turner, and Cepko, 1987), and COS-7 cells (ATCC CRL-1651) were cultured in Dulbecco's Modified Eagle medium (DMEM; Gibco BRL, Gaithersburg, MD) with 10% bovine calf serum (Hyclone Labs Inc., Logan, UT) containing 100 U/mL penicillin and 100 µg/mL streptomycin (GIBCO BRL) (Dhawan et al., 1991). Virus-containing medium was harvested from sub-confluent cultures of the virus-producing cell line, filtered through 0.45 µm syringe filters (Millipore), stored at 4 °C or frozen on pulverized dry ice and stored at −80 °C.

Retrovirus concentration

Retrovirus was concentrated by adding PEG 8000 (Sigma-Aldrich) to a final concentration of 8% (w/v), followed by overnight incubation at 4 °C and centrifugation at 1500 *g* for 45 min. The pellet was resuspended in phosphate-buffered saline pH = 7.4 (PBS) and dialyzed overnight against PBS (cut off 300 kD) for Circular Dichroism analysis, SDS-PAGE, and two-dimensional SDS-PAGE. The pellet was resuspended in fresh medium for the transduction assays. The integrity of virus particles was verified by using a Zeta Plus light scattering instrument (Brookhaven Instruments) and transduction assay.

Transduction efficiency assay

Transduction of the LacZ virus was measured by a microplate assay (36). The day before transduction with the LacZ virus, a 10 cm dish of confluent 3T3 cells was treated with trypsin and the cells obtained were counted with a Coulter counter model ZM (Coulter Electronics, Hialeah, FL). Five thousand cells in 100 μL medium per well were plated in a 96-well, flat-bottom tissue culture dish with a low-evaporation lid (Costar, Cambridge, MA) and growth at 37 °C, 10% CO_2. The next day (16–24 h later), the medium was removed and a LacZ-virus solution containing polybrene (Sigma-Aldrich) at a final concentration of 8 μg/mL was added to the cells. Two days after transduction, the culture medium was removed and the cells were washed with PBS. The cells were lysed with 50 μL of lysis buffer (PBS with 1 mM $MgCl_2$ and 0.5% Nonidet P-40) and incubated at 37 °C. After 30 min, 50 μL of lysis buffer containing 6 mM *ortho*-nitrophenyl β-ᴅ-galactopyranoside (ONPG, Sigma-Aldrich) warmed to 37 °C was added to each well, and the plate was incubated at 37 °C for 45 min. The reactions were stopped by the addition of 20 μL of stop buffer (1 M Na_2CO_3). The plate was brought to room temperature and the absorbance at 420 nm (A_{420}) was measured in a plate reader (Molecular Devices, Menlo Park, CA). Background corrections were performed at 650 nm.

Production of virus mutants

Three plasmids (pVPack vectors: pVPackEco, pVPack-GP and pFB-Neo-LacZ) carrying viral genes were purchased from Stratagene. The three pVPack plasmids were co-transfected in a COS-7 cell line using a mammalian transfection kit (Stratagene) following the manufacturer's instructions. In brief, COS-7 cells were seeded in 6-well plates at 60–70% confluence a day before transfection. Two micrograms of each plasmid were co-transfected and after 12–24 h, cells were washed twice with PBS and fresh medium was added. Virus was harvested 12–24 h after the washing step and every 12 h thereafter for the next 5 days. Virus production was followed using RT-PCR. Samples were prepared by heating 100 μL of virus solution at 95 °C for 15 min; 1 μl of sample was used as a template in the reaction and was amplified using the One Step RT-PCR kit from Qiagen. PCR without a reverse transcription step was performed to detect possible residual or carry over plasmid DNA (derived from the transfection procedure) in the virus samples. Protease and reverse transcriptase mutants were created using the QuikChange mutagenesis kit (Stratagene) following the manufacturer's directions. Reverse transcriptase mutants were designed based on the work of Blain and Goff (1993). The primers used for the mutagenesis were the following: R657S forward: gaccaagcggcctgcaaggcagccatcacag; R657S reverse: ctgtgatggctgccttgcaggccgcttggtc; D524N forward: gacgccgaccacacctggtacacgaatggaagcagtctcttac; D524N reverse: gtaagagactgcttccattgtgtaccaggtgtggtcggcgtc; Y586F forward: gtttatactgatagccgttttgcttttgctactgcccatatccatgg; Y586F reverse: ccatggatatgggcagtagcaaaagcaaaacggctatcagtataaac.

The protease defective (PR−) mutant was created based on the work of Fu et al. (2006) using the following primers: D27N forward:

cgtcaccttcctggtaaatactggggcccaacactccg; D27N reverse: cggagtgttgggccccagtatctaccaggaaggtgacg. All mutations were within the *gag-pol* gene present in the pVPack-GP plasmid, and mutations were confirmed by DNA sequencing analysis. Wild type virus was produced using the non-mutated pVPack-GP plasmid and used as a control in all the experiments in comparing the mutants. We compared the bioactivity of the PR⁻ retrovirus with wild type produced under the same conditions, and we confirmed that there was no bioactivity for the PR⁻ mutated virus.

Circular dichroism

CD analysis was performed on virus samples in PBS with an AVIV 202 CD spectrophotometer (AVIV Biomedical) using a cuvette with path length of 0.1 cm. Samples were incubated at 37 °C for 13 h and spectra were automatically collected every hour in the range 200 to 320 nm, with a step size of 0.2 nm.

Two-dimensional gel electrophoresis

Briefly, 50 μg of total proteins from each sample was mixed with 125 μl of rehydration buffer containing 8 M urea, 2% CHAPS, 10 mM DTT and 0.2% (pH 3–10) carrier ampholytes, and then loaded overnight onto linear pH 3–6 or pH 5–8 IPG strips through passive in-gel rehydration. After isoelectric focusing with a maximum of 5000 V for a total of 12,000 Vh at 20 °C and equilibrating first in a DTT buffer (15 min, 6 M urea, 2% (w/v) SDS, 0.5 M Tris/HCl, pH 6.8, and 1% DTT), and then in an iodoacetamide buffer (15 min, 6 M urea, 2% SDS, 0.5 M Tris/HCl, pH 6.8, and 2.5% iodoacetamide), the IPG strips were positioned on 10–15% (w/v) polyacrylamide gels for the second-dimension separation at 200 V. The gel was stained with SyproRuby fluorescent dye according to the manufacturer's instructions (Molecular Probes, Eugene, OR, U.S.A.). The stained gel was scanned with a Fluor-S MultiImager system (Bio-Rad) and analysed with PDQuest software (version 7.0; Bio-Rad).

SDS-PAGE analysis

Briefly, 50 μg of total protein from each sample was mixed with sample buffer to a final concentration of 1× according to standard procedures and loaded on a 4–20% Precision precast polyacrylamide gel (Pierce). After separation the gel was stained with Coomassie blue.

End point and real time RT-PCR

MMuLV-based α-SGC-LacZ-virus solution produced from stable packaging cell line was incubated at 37 °C, and samples were collected at different time points and frozen for later RNA purification. Virus was concentrated by PEG 8000 precipitation and RNA from each sample was purified using QIAamp Viral RNA Minikit (Qiagen), and quantified by absorption at 260 nm. For each sample a 5 ng/μL solution was prepared and used for end point and real time RT-PCR using the following primers: Gag forward: ccaggtaaactgacagctctgatcgagtctg; Gag reverse: ggcccttgtgttattccttttaccttgg; LacZ forward: ggtctgctgctgctgaacgg; LacZ reverse: atcgacagatttgatccagcgatacag. For each set of primers a product of 200 base pairs is expected. End point PCR was carried out on Mastercycler Epgradient-S (Eppendorf), using the One Step RT-PCR kit (Qiagen). The reactions were prepared following the manufacturer's instructions and using 5 ng total RNA as a template for 30 cycles. Semi-quantitative analysis of the product was performed using Quantity One software (Biorad).

The Natural Endogenous Reverse Transcription (NERT) was investigated incubating the virus at 37 °C and 4 °C. Samples collected at different time points were heated at 95 °C for 15 min and 2 μL of the samples, without RNA extraction, were used as template in PCR reaction without reverse transcription step. The amplification

reactions were carried out for 40 cycles and semi-quantitative analysis of the product was performed using Quantity One software.

Real time PCR was performed on a Light Cycler LC-24 (Idaho Technology), using Omniscript and Sensiscript RT Kits (Qiagen) for the reverse transcription reaction step and SuperScript III Platinum CellsDirect Two-Step qRT-PCR Kits (Invitrogen) for quantitative PCR. For reverse transcription, 5 ng of total RNA was used as template. For real time amplification, 1 µL of the reverse transcription reactions was used as template. Because of the small volumes of viral mutants and wild type control produced from transient transfection of COS-7 cell, samples for PCR analysis were prepared following a different protocol: samples collected for decay experiments at 37 °C were heated at 95 °C for 15 min. For end point RT-PCR and the reverse transcription step, 2 µL of the sample without RNA extraction were used. For real time PCR, 2 µL of the ten-fold diluted reverse transcription reactions was used; for PCR analysis of mutants, primers specific for the LacZ region were used. All reactions were performed according to the manufacturer's instructions. A calibration curve was obtained using the pFB-Neo-LacZ plasmid as template. Data obtained by real time PCR were fitted using exponential decay model.

Northern blot

Virus solutions previously harvested and frozen at −80 °C were thawed and incubated at 37 °C over a period of 24 h. Samples, taken at the beginning of the incubation (time zero) and after 24 h, were subsequently stored at 4 °C. Virus particles were concentrated by ultracentrifugation at 32,000 rpm for 1 h and 30 min and RNA was extracted and quantified by UV absorbance. RNA samples were first denatured at 70 °C for 15 min in formaldehyde buffer (Formaldehyde Sample Buffer, 5 X Cambrex) and then separated by 1.25% agarose gel (Reliant Precast gels, Cambrex) in Mops buffer (Cambrex) at 70 V for 3 h. RNA was transfer by vacuum blotting on positively charged nylon membrane (BrightStar®-Plus, Ambion) in 2× SSC buffer and cross-linked at 80 °C for 2 h. Prehybridization was performed at 40 °C for 30 min in ULTRAhyb® Ultrasensitive Hybridization Buffer (Ambion). The 50 base pair probe was radiolabeled with ^{32}P (Rediprime II, Amersham) following the manufacturer's instructions and denatured at 90 °C for 10 min before being added to the membrane. Hybridization was performed overnight at 40 °C. After hybridization, blot was washed three times for 15 min at 55 °C with a solution containing 2× SSC and 0.1% SDS. Damp blots were wrapped in plastic wrap and exposed to PhosphoImager screen for 1 h and visualized on a GE Typhoon Imager.

References

Aiuti, A., Slavin, S., Aker, M., Ficara, F., Deola, S., Mortellaro, A., Morecki, S., Andolfi, G., Tabucchi, A., Carlucci, F., Marinello, E., Cattaneo, F., Vai, S., Servida, P., Miniero, R., Roncarolo, M.G., Bordignon, C., 2002. Correction of ADA-SCID by stem cell gene therapy combined with nonmyeloablative conditioning. Science 296 (5577), 2410–2413.

Ausar, S.F., Espina, M., Brock, J., Thyagarayapuran, N., Repetto, R., Khandke, L., Middaugh, C.R., 2007. High-throughput screening of stabilizers for respiratory syncytial virus: identification of stabilizers and their effects on the conformational thermostability of viral particles. Hum. Vaccin. 3 (3), 94–103.

Ausar, S.F., Rexroad, J., Frolov, V.G., Look, J.L., Konar, N., Middaugh, C.R., 2005. Analysis of the thermal and pH stability of human respiratory syncytial virus. Mol. Pharm. 2 (6), 491–499.

Barquinero, J., Eixarch, H., Perez-Melgosa, M., 2004. Retroviral vectors: new applications for an old tool. Gene Ther. 11 (Suppl 1), S3–S9.

Beer, C., Meyer, A., Muller, K., Wirth, M., 2003. The temperature stability of mouse retroviruses depends on the cholesterol levels of viral lipid shell and cellular plasma membrane. Virology 308 (1), 137–146.

Ben-Artzi, H., Zeelon, E., Gorecki, M., Panet, A., 1992. Double-stranded RNA-dependent RNase activity associated with human immunodeficiency virus type 1 reverse transcriptase. Proc. Natl. Acad. Sci. U. S. A. 89 (3), 927–931.

Blain, S.W., Goff, S.P., 1993. Nuclease activities of Moloney murine leukemia virus reverse transcriptase. Mutants with altered substrate specificities. J. Biol. Chem. 268 (31), 23585–23592.

Cantor, Schimmel, 1980. Biophysical Chemistry." 2 — Part II: Techniques For The Study Of Biological Structure And Function. Freeman. 3 vols.

Cavazzana-Calvo, M., Hacein-Bey, S., de Saint Basile, G., Gross, F., Yvon, E., Nusbaum, P., Selz, F., Hue, C., Certain, S., Casanova, J.L., Bousso, P., Deist, F.L., Fischer, A., 2000. Gene therapy of human severe combined immunodeficiency (SCID)-X1 disease. Science 288 (5466), 669–672.

Chuck, A.S., Clarke, M.F., Palsson, B.O., 1996. Retroviral infection is limited by Brownian motion. Hum. Gene Ther. 7 (13), 1527–1534.

Cosset, F.L., Takeuchi, Y., Battini, J.L., Weiss, R.A., Collins, M.K., 1995. High-titer packaging cells producing recombinant retroviruses resistant to human serum. J. Virol. 69 (12), 7430–7436.

D'Souza, V., Summers, M.F., 2004. Structural basis for packaging the dimeric genome of Moloney murine leukaemia virus. Nature 431 (7008), 586–590.

Daly, G., Chernajovsky, Y., 2000. Recent developments in retroviral-mediated gene transduction. Mol. Ther. 2 (5), 423–434.

Danos, O., Mulligan, R.C., 1988. Safe and efficient generation of recombinant retroviruses with amphotropic and ecotropic host ranges. Proc. Natl. Acad. Sci. U. S. A. 85 (17), 6460–6464.

Davis, H.E., Morgan, J.R., Yarmush, M.L., 2002. Polybrene increases retrovirus gene transfer efficiency by enhancing receptor-independent virus adsorption on target cell membranes. Biophys. Chem. 97 (2–3), 159–172.

Davis, H.E., Rosinski, M., Morgan, J.R., Yarmush, M.L., 2004. Charged polymers modulate retrovirus transduction via membrane charge neutralization and virus aggregation. Biophys. J. 86 (2), 1234–1242.

Dhawan, J., Pan, L.C., Pavlath, G.K., Travis, M.A., Lanctot, A.M., Blau, H.M., 1991. Systemic delivery of human growth hormone by injection of genetically engineered myoblasts. Science 254 (5037), 1509–1512.

Fu, W., Dang, Q., Nagashima, K., Freed, E.O., Pathak, V.K., Hu, W.S., 2006. Effects of Gag mutation and processing on retroviral dimeric RNA maturation. J. Virol. 80 (3), 1242–1249.

Fu, W., Rein, A., 1993. Maturation of dimeric viral RNA of Moloney murine leukemia virus. J. Virol. 67 (9), 5443–5449.

Garret, and Grisham (1995). Nucleotides and Nucleic Acids. *In* "Biochemistry" (S.c Publishing, Ed.),pp. 199-202.

Goff, S.P., 1990. Retroviral reverse transcriptase: synthesis, structure, and function. J. Acquir. Immune Defic. Syndr. 3 (8), 817–831.

Gordon, E.M., Anderson, W.F., 1994. Gene therapy using retroviral vectors. Curr. Opin. Biotechnol. 5 (6), 611–616.

Hanenberg, H., Xiao, X.L., Dilloo, D., Hashino, K., Kato, I., Williams, D.A., 1996. Colocalization of retrovirus and target cells on specific fibronectin fragments increases genetic transduction of mammalian cells. Nat. Med. 2 (8), 876–882.

Hibbert, C.S., Rein, A., 2005. Preliminary physical mapping of RNA–RNA linkages in the genomic RNA of Moloney murine leukemia virus. J. Virol. 79 (13), 8142–8148.

Jacobo-Molina, A., Arnold, E., 1991. HIV reverse transcriptase structure–function relationships. Biochemistry 30 (26), 6351–6356.

Kohl, N.E., Emini, E.A., Schleif, W.A., Davis, L.J., Heimbach, J.C., Dixon, R.A., Scolnick, E.M., Sigal, I.S., 1988. Active human immunodeficiency virus protease is required for viral infectivity. Proc. Natl. Acad. Sci. U. S. A. 85 (13), 4686–4690.

Kohn, D.B., Sadelain, M., Dunbar, C., Bodine, D., Kiem, H.P., Candotti, F., Tisdale, J., Riviere, I., Blau, C.A., Richard, R.E., Sorrentino, B., Nolta, J., Malech, H., Brenner, M., Cornetta, K., Cavagnaro, J., High, K., Glorioso, J., 2003. American Society of Gene Therapy (ASGT) ad hoc subcommittee on retroviral-mediated gene transfer to hematopoietic stem cells. Mol. Ther. 8 (2), 180–187.

Kotani, H., Newton 3rd, P.B., Zhang, S., Chiang, Y.L., Otto, E., Weaver, L., Blaese, R.M., Anderson, W.F., McGarrity, G.J., 1994. Improved methods of retroviral vector transduction and production for gene therapy. Hum. Gene Ther. 5 (1), 19–28.

Kwon, Y.J., Peng, C.A., 2005. High-yield retroviral production using a temperature-modulated two-stage operation. Biotechnol. Bioeng. 90 (3), 365–372.

Le Doux, J.M., Davis, H.E., Morgan, J.R., Yarmush, M.L., 1999. Kinetics of retrovirus production and decay. Biotechnol. Bioeng. 63 (6), 654–662.

Le Doux, J.M., Morgan, J.R., Snow, R.G., Yarmush, M.L., 1996. Proteoglycans secreted by packaging cell lines inhibit retrovirus infection. J. Virol. 70 (9), 6468–6473.

Le Doux, J.M., Morgan, J.R., Yarmush, M.L., 1998. Removal of proteoglycans increases efficiency of retroviral gene transfer. Biotechnol. Bioeng. 58 (1), 23–34.

Le Doux, J.M., Morgan, J.R., Yarmush, M.L., 1999. Differential inhibition of retrovirus transduction by proteoglycans and free glycosaminoglycans. Biotechnol. Prog. 15 (3), 397–406.

Lim, D., Gregorio, G.G., Bingman, C., Martinez-Hackert, E., Hendrickson, W.A., Goff, S.P., 2006. Crystal structure of the moloney murine leukemia virus RNase H domain. J. Virol. 80 (17), 8379–8389.

Mason, J.M., Guzowski, D.E., Goodwin, L.O., Porti, D., Cronin, K.C., Teichberg, S., Pergolizzi, R.G., 1999. Human serum-resistant retroviral vector particles from

galactosyl (alpha1–3) galactosyl containing nonprimate cell lines. Gene Ther. 6 (8), 1397–1405.

Merten, O.W., Cruz, P.E., Rochette, C., Geny-Fiamma, C., Bouquet, C., Goncalves, D., Danos, O., Carrondo, M.J., 2001. Comparison of different bioreactor systems for the production of high titer retroviral vectors. Biotechnol. Prog. 17 (2), 326–335.

Miller, D.G., Adam, M.A., Miller, A.D., 1990. Gene transfer by retrovirus vectors occurs only in cells that are actively replicating at the time of infection. Mol. Cell Biol. 10 (8), 4239–4242.

Mitani, K., Wakamiya, M., Caskey, C.T., 1993. Long-term expression of retroviral-transduced adenosine deaminase in human primitive hematopoietic progenitors. Hum. Gene Ther. 4 (1), 9–16.

Murti, K.G., Bondurant, M., Tereba, A., 1981. Secondary structural features in the 70S RNAs of Moloney murine leukemia and Rous sarcoma viruses as observed by electron microscopy. J. Virol. 37 (1), 411–419.

Pages, J.C., Bru, T., 2004. Toolbox for retrovectorologists. J. Gene Med. 6 (Suppl 1), S67–S82.

Paul, R.W., Morris, D., Hess, B.W., Dunn, J., Overell, R.W., 1993. Increased viral titer through concentration of viral harvests from retroviral packaging lines. Hum. Gene Ther. 4 (5), 609–615.

Pensiero, M.N., Wysocki, C.A., Nader, K., Kikuchi, G.E., 1996. Development of amphotropic murine retrovirus vectors resistant to inactivation by human serum. Hum. Gene Ther. 7 (9), 1095–1101.

Pham, L., Ye, H., Cosset, F.L., Russell, S.J., Peng, K.W., 2001. Concentration of viral vectors by co-precipitation with calcium phosphate. J. Gene Med. 3 (2), 188–194.

Poryvaev, V.D., 1995. A thermodynamic analysis of oxidative inactivation of influenza virus and lipid peroxidation of viral envelope lipids. Vopr. Virusol. 40 (6), 273–276.

Poryvaev, V.D., Viatkina, T.G., Ryzhikov, A.B., Sergeev, A.N., Iagofarov, S.R., 1996. Effect of components of virus-containing allantoic fluid on the stability of influenza virus during storage. Vopr. Virusol. 41 (3), 126–129.

Poryvaev, V.D., Zykova, N.A., 1995. The effect of conditions of storage and composition of viral material on lipid peroxidation of the viral envelope and inactivation of the influenza virus. Vopr. Virusol. 40 (2), 62–65.

Price, J., Turner, D., Cepko, C., 1987. Lineage analysis in the vertebrate nervous system by retrovirus-mediated gene transfer. Proc. Natl. Acad. Sci. U. S. A. 84 (1), 156–160.

Reeves, L., Cornetta, K., 2000. Clinical retroviral vector production: step filtration using clinically approved filters improves titers. Gene Ther. 7 (23), 1993–1998.

Relph, K., Harrington, K., Pandha, H., 2004. Recent developments and current status of gene therapy using viral vectors in the United Kingdom. BMJ 329 (7470), 839–842.

Riggin, C.H., Bondurant, M., Mitchell, W.M., 1975. Physical properties of Moloney murine leukemia virus high-molecular-weight RNA: a two subunit structure. J. Virol. 16 (6), 1528–1535.

Robbins, P.D., Ghivizzani, S.C., 1998. Viral vectors for gene therapy. Pharmacol. Ther. 80 (1), 35–47.

Roe, T., Reynolds, T.C., Yu, G., Brown, P.O., 1993. Integration of murine leukemia virus DNA depends on mitosis. Embo. J. 12 (5), 2099–2108.

Takeuchi, Y., Porter, C.D., Strahan, K.M., Preece, A.F., Gustafsson, K., Cosset, F.L., Weiss, R.A., Collins, M.K., 1996. Sensitization of cells and retroviruses to human serum by (alpha 1–3) galactosyltransferase. Nature 379 (6560), 85–88.

Traktman, P., Baltimore, D., 1982. Protease bypass of temperature-sensitive murine leukemia virus maturation mutants. J. Virol. 44 (3), 1039–1046.

Vu, H.N., Ramsey, J.D., Pack, D.W., 2007. Engineering of a stable retroviral gene delivery vector by directed evolution. Mol. Ther.

Witte, O.N., Baltimore, D., 1978. Relationship of retrovirus polyprotein cleavages to virion maturation studied with temperature-sensitive murine leukemia virus mutants. J. Virol. 26 (3), 750–761.

Zhang, H., Duan, L.X., Dornadula, G., Pomerantz, R.J., 1995. Increasing transduction efficiency of recombinant murine retrovirus vectors by initiation of endogenous reverse transcription: potential utility for genetic therapies. J. Virol. 69 (6), 3929–3932.